Isothermal Bistability Due to Remote Control: A Model for Selective Catalytic Oxidation

Timm Rebitzki, Bernard Delmon, and Jochen H. Block
Fritz-Haber-Institut der Max-Planck-Gesellschaft, Faradayweg 4-6, D-14195 Berlin, Germany

Special kinetic behaviors in isothermal reactions on heterogeneous catalysts composed of two components with different roles are studied with the focus on bistabilities that could occur in stirred-tank flow reactors when control of catalytic sites on one component by mobile (spillover) species produced by the other operates. The comprehensive kinetic model involves: (1) generation of spillover species on the second phase, their transfer to the potentially catalytic phase, and their reaction with this acceptor to generate selective sites; (2) the kinetics of the catalytic reaction. We developed a model for selective catalytic oxidation, where catalyst sites change from nonselective to selective under the influence of the control by spillover oxygen. The model is based on the system of differential equations. By integration and iteration to the steady state for each value of the external control parameter under investigation, the oxygen and hydrocarbon reactant consumption, as well as the state of the catalyst, is calculated. These calculations predict bistable selectivity for certain ranges of concentration in the feed. Data on the boundaries of the hysteresis loops as a function of catalyst composition and oxygen partial pressure are discussed, as well as the variation of these hysteresis boundaries as a function of the internal parameters.

Introduction

Most selective oxidation catalysts used in industry reveal two or, more often, several distinct solid phases. These phases cooperate with each other to bring about synergetic effects (Weng and Delmon, 1992; Delmon, 1993). The main aspects of this cooperation, namely increased selectivity, activity, and resistance to aging, can be explained by the remote control mechanism (Delmon and Matralis, 1991).

Classic explanations concerning cooperation or synergy between components in heterogeneous catalysts are (1) formation of new compounds by solid-state reaction, (2) mutual contamination by surface migration of components of one phase onto the surface of the other, and (3) bifunctional catalysis. In bifunctional catalysis, a reactant undergoes a partial reaction on one phase, desorbs from that phase, and adsorbs on the second phase where it undergoes the final reaction. The remote control mechanism is very different from this mechanism and brings about strong synergies between phases. It does not correspond to the solid-state reaction nor contamination. The reactant undergoes full chemical transformation on one of the two phases ("acceptor"). The key feature of the remote control is that a surface mobile species produced on another component of the catalyst ("donor") chemically reacts with the surface of the acceptor to transform inactive or nonselective sites to active selective ones (Weng and Delmon, 1992; Delmon, 1993). In selective catalytic oxidation, some oxides (donors) are indeed able to dissociate molecular oxygen to form a surface mobile species O_{so}. This species migrates on the surface of the donor and "spills over" onto the surface of the acceptor. Acceptors have the potential to carry active and selective sites, provided some reaction with the spillover species O_{so} takes place. Once they are activated, the active sites transform a large number of molecules until some accident occurs, probably the fact that a molecule follows a wrong reaction path occurring with a

Correspondence concerning this article should be addressed to B. Delmon, who is currently at Université Catholique de Louvain, Unité de Catalyse et Chimie des Matériaux Divisés, Place Croix du Sud, 2 Boîte 17, 1348 Louvain-la-Neuve, Belgium.

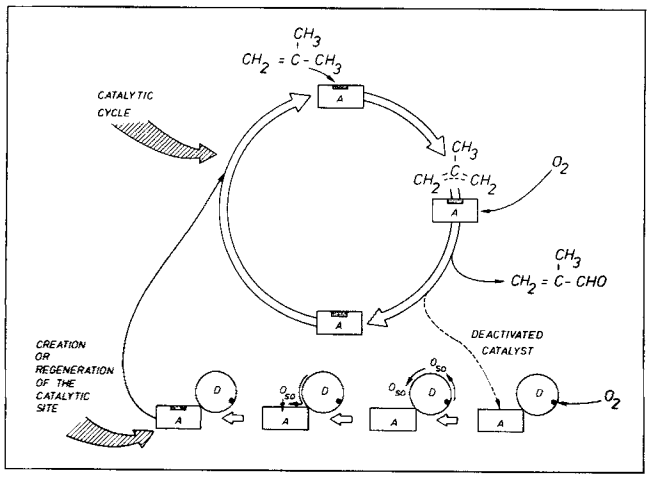

Figure 1. Remote-controlled reaction.

low, but not negligible, probability. The site thus becomes nonselective. (In allylic oxidation, this may be linked to some overreduction of the site.) The deactivated, nonselective site can be activated again by O_{so}. The overall process is represented in the lower part of Figure 1. It corresponds to a *control* of catalytic site through signals (O_{so}) coming from a (relatively) *remote* separate phase. The upper part represents the catalytic cycle, operating as long as the activated sites remain active.

In accordance with many observations, the model presented herein describes a given catalyst (or part of it, or, at an even smaller scale, a given site) as exhibiting two states. We had predicted that this ability to exist in two states could lead to oscillatory behavior, namely oscillation between these two states. A calculation with a simplified model indeed indicated the possibility of obtaining damped oscillations (Delmon and Matralis, 1991). Along the same line, this could constitute good reason for expecting bistability. One could indeed imagine that, under exactly the same reaction conditions, the same catalyst can exhibit two different activity patterns according to its previous history. In the frame of our model, a catalyst in the nonselective state consumes more oxygen, because it completely degrades hydrocarbons to CO_2 and H_2O. Less oxygen thus remains in the gas phase, less O_{so} is produced, and thus fewer selective catalytic sites are formed; this leads to a stable nonselective state. Conversely, even with an identical supply of oxygen to the reactor, a catalyst in the selective state leaves more unreacted oxygen in the gas phase and thus permits the continuous formation or regeneration of selective sites. Although not formally demonstrated, the existence of bistabilities is strongly suggested by unexplained episodes during catalytic tests, where catalysts, after having worked efficiently, suddenly lose selectivity; the opposite may also occur. This phenomenon has often been observed by industrial scientists, typically in the case of the oxidation of butane to maleic anhydride, and also in the oxidation of toluene to benzaldehyde, as confirmed by the experience of Delmon (1969).

The present article demonstrates theoretically that reactions in which a remote control occurs exhibit bistability in certain reactor conditions. To our knowledge, the remote control is, among the various explanations of synergy between catalyst components (especially bifunctional catalysts), the only one potentially leading to bistability in isothermal conditions. The model is the most advanced one presented until now. It is completely rigorous. The kinetics of all the steps postulated by the remote control are included in the model; these steps have been considered at the exclusion of any other elementary process. It should be underlined that the calculations assume that no *thermal effects* occur. The origin of the bistability is thus completely different from the well-known effect of temperature runoff observed in oxidation reactions, which can also lead to some sort of bistability and even nonisothermal oscillations. It is also different from those detected in CO oxidation or similar reactions, where one single metal surface is involved and unusual adsorption equations and special kinetics of reactions between adsorbed species are the origin of the phenomena.

The results stem from a comprehensive mathematical model involving both the dynamics of the remote control loop (lower part of Figure 1) and the kinetics of the catalytic reaction (upper part of Figure 1). The starting point was a much simpler model, based on pseudo-steady-state equations developed previously (Melo Faus et al., 1991). The model was aimed at accounting for the changes of activity observed in an *oxygen-aided* reaction, namely the dehydration of *N*-ethyl-formamide to propionitrile on two-phase Sb_2O_4–MoO_3 mixtures (Melo Faus et al., 1991; Zhou et al, 1991a,b). This model gave with a high accuracy ($\pm 5\%$) the yields in nitrile on 21 Sb_2O_4–MoO_3 mixtures of different composition, for oxygen pressures ranging from 0.3 to 45 torr and three different temperatures (350, 370 and 390°C). The essential differences in the present model are that (1) as in all oxidation processes, two reactions can take place, namely a selective and a nonselective one; and (2) the differential equations corresponding to the flow of spillover oxygen assuring the remote control, as well as those describing the rates of reaction and the dynamics in the flow reactor, are taken into account. The reactor (Figure 2) is a continuously stirred tank. We can thus represent non-steady-state (or transient) phenomena as well as steady-state processes. The model permits a study of the influence of the kinetic constants on which the catalyst and reaction depend (internal parameters):

- Detailed kinetics of the remote control loop, in particular the response time of the remote control process
- Relative rates of the selective and nonselective reaction
- Orders of these reactions with respect to the reactant and to oxygen
- Activation energies.

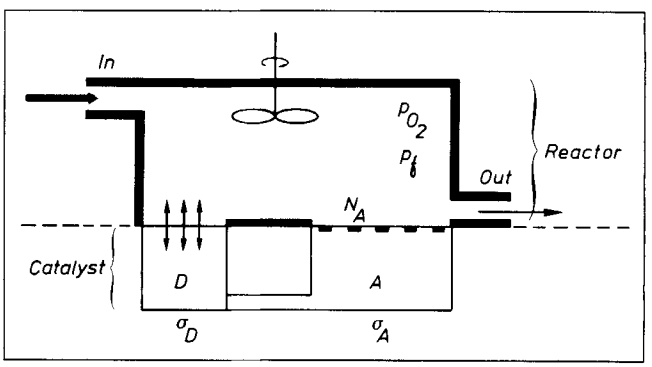

Figure 2. Stirred tank reactor as assumed in the model.

The external parameters are the fluxes of hydrocarbon reactant and oxygen into the flow reactor and the composition of the catalyst mixture.

We have not explicitly investigated the influence of the activation energy or the influence of temperature: both can be deduced from variations of the individual rate constants. We shall describe the model in detail in the following section.

Oxygen flux (or partial pressure) is the crucial parameter. Most figures summarizing the results will thus concern the influence of this parameter. A typical case will show how the various characteristic quantities (variables of the model system) in a given reaction vary as a function of the flux. The other illustrations will focus on the domains where a bistability exists. They will summarize the trends observed with change in external (such as hydrocarbon reactant, partial pressure, catalyst composition) or internal parameters (as mentioned earlier).

Basis of the Mathematical Model

The model is based on the general reaction scheme valid for all selective oxidation reactions, namely a competition between a selective path and a nonselective one, leading to H_2O and CO_2 (sometimes some CO). A typical allylic reaction, namely the oxidation of propene to acrolein, gives an excellent picture of the phenomena:

$$CH_2=CH-CH_3 \begin{cases} \text{selective} \\ +O_2 \rightarrow CH_2=CH-CHO+H_2O \\ +4.5\ O_2 \rightarrow 3\ CO_2+3\ H_2O \\ \text{nonselective} \end{cases}$$

In order to model the activity and selectivity of a reaction when a remote control operates, it is necessary and sufficient to break down the overall phenomena into five elementary steps (Eqs. 1a to 1e). Two additional expressions represent the catalytic reaction of the selective and nonselective sites:

$$O_2+2\,D \rightarrow 2\,OD \quad \text{(production of } O_{so}) \tag{1a}$$

$$O_2+2\,D \leftarrow 2\,OD \quad \text{(recombination of } O_{so}) \tag{1b}$$

$$OD \leftrightarrows OA \quad \text{(transfer between donor and acceptor)} \tag{1c}$$

$$OA+B \rightarrow S \quad \text{(reaction of } O_{so} \text{ with nonselective site)} \tag{1d}$$

$$M+S \rightarrow M'+B \quad \text{(deactivation site during a deactivating side reaction of reactant M)} \tag{1e}$$

$$(M)+(O_2)+S \rightarrow S+ \text{selective oxidation product (selective catalytic reaction)} \tag{1f}$$

$$(M)+(O_2)+B \rightarrow B+(CO_2)+(H_2O) \quad \text{(nonselective catalytic reaction)} \tag{1g}$$

Equations 1a and 1b describe the dissociative adsorption of molecular oxygen from the gas phase onto the donor and the corresponding reverse reaction (D is an unoccupied site, OD spillover oxygen on the donor). The transfer of spillover oxygen between donor and acceptor is represented in Eq. 1c. Spillover oxygen *OA* is a mobile species present on the acceptor surface that is not associated with a particular surface site. Equation 1d reflects the reaction of spillover oxygen with a nonselective acceptor site B, transforming that site to one that is selective (S) for the reaction with the reactant molecule M. Equation 1e illustrates a reaction "gone wrong," that is, when a site has become nonselective, yielding, in general, an altered reactant molecule M'. Finally Eqs. 1f and 1g summarize the overall reaction of reactant M with oxygen in the selective and nonselective case, respectively. For the present model it is not necessary to describe in detail the intermediate reaction steps involved in these two reactions. We therefore do not assume at this stage any specific stoichiometry for the reactions represented by these equations. In the overall selective reaction Eq. 1f, N_S molecules of oxygen are consumed for every molecule of reactant M, while N_B are consumed in the nonselective reaction (Eq. 1g).

The mathematical description of the remote control process itself (Eqs. 1a to 1e) consists of a system of five ordinary differential equations, each of which relates the time derivative of a system variable to the sum of several rate terms that affect the increase or decrease of that system variable. The seven rate terms are a direct counterpart of the chemical equations described earlier. To facilitate an overview of the equations these terms are summarized below.

Rate Term	Description	Unit	
$R_d = k_d p_{O_2}(1-\theta_D)^2(1-r)\sigma_D$	Dissociation	1/s	(2a)
$R_d^- = k_d^- \theta_D^2(1-r)\sigma_D$	Recombination	1/s	(2b)
$R_t = k_t(\theta_D-\theta_A)Qr\sigma_A(1-r)\sigma_D$	Transfer	1/s	(2c)
$R_a = k_a a(1-\alpha)\theta_A r\sigma_A$	Activation	1/s	(2d)
$R_a^- = k_a^- a p_f \alpha r\sigma_A$	Deactivation	1/s	(2e)
$R_S = k_S a\alpha r\sigma_A p_f^{m_1} p_{O_2}^{m_2}$	Selective reaction	torr/s	(2f)
$R_B = k_B a(1-\alpha)r\sigma_A p_f^{m_3} p_{O_2}^{m_4}$	Nonselective (burn) reaction	torr/s	(2g)

The five system variables are partial pressures of the hydrocarbon reactant p_f and oxygen p_{O_2} in the reactor (namely also at the outlet), the spillover oxygen coverage on donor and acceptor θ_D and θ_A, and the fraction of active sites on the acceptor surface α. The constants that were not changed in the calculations include the specific surface area of donor and acceptor, σ_D and σ_A, the contact quality of donor particles with acceptor particles in the catalyst mixture, which controls the transfer of spillover oxygen, Q, and the maximum density a of active sites on the surface of the acceptor phase; r is the catalyst composition, expressed as the mass ratio of acceptor to donor components of catalyst. Integers m_i describe the reaction order with respect to hydrocarbon reactant and oxygen for both types of reactions. The system of ordinary differential equations may then be written as follows (a dot over a symbol indicates the time derivative):

$$\dot{\theta}_D = R_d - R_d^- - R_t \tag{3a}$$

$$\dot{\theta}_A = R_t - R_a \tag{3b}$$

$$\dot{\alpha} = R_a - R_a^- \tag{3c}$$

$$\dot{p}_f = F/V(\bar{p}_f - p_f) - R_S - R_B \tag{3d}$$

$$\dot{p}_{O_2} = F/V(\bar{p}_{O_2} - p_{O_2}) - N_S R_S - N_B R_B \tag{3e}$$

Calculation Methods

For the discussion of the phenomenon of bistability, we will define some terms. For the sake of clarity, only the variation of the feed oxygen partial pressure $\bar{p}_{O_2}$ with constant hydrocarbon reactant pressure in the feed $\bar{p}_f$ and catalyst composition r will be considered in the following; we also exclude the more complex behavior associated with oscillations. The boundaries between the regions of monostability and bistability are then defined as follows. The reactor as a whole can exist in exactly two *steady* states, namely selective S or nonselective B (for burn). During the slow increase of the oxygen pressure, state B may become unstable and the system perform a rapid transition to the selective state S. The point (oxygen pressure) at which this occurs is termed $\tau_B(\bar{p}_f,r)$. Conversely, a slow decrease of the oxygen partial pressure may lead to a loss of stability for the state S at $\tau_S(\bar{p}_f,r)$ where the system rapidly returns to the nonselective state B. Three regions are then determined by the corresponding ranges of $\bar{p}_{O_2}$ as follows: For $\bar{p}_{O_2} \le \tau_S(\bar{p}_f,r)$ there is one and only one stable steady state with low selectivity (monostable region B). Likewise, for $\bar{p}_{O_2} \ge \tau_B(\bar{p}_f,r)$ only the steady state with high selectivity (monostable region S) exists. Since in general $\tau_B > \tau_S$, there is a third intermediate region of finite width $\Delta = \tau_B - \tau_S$ in which two stable states with widely differing selectivity may be attained (bistability region). Δ thus refers to the width of the hysteresis.

The precision of the positions in the phase space of the hysteresis transitions were calculated directly from the plots of the data produced during the parameter ramping. To produce these plots, a control parameter (typically the oxygen or hydrocarbon reactant partial pressure) is written as a function of time such that the parameter performs one cycle of a sawtooth wave (increases linearly from a low to a high value and back again to the low value) in a given amount of time T_c. Before ramping the parameter, the system of differential equations is integrated outside the bistable region at the starting value of the parameter and thus allowed to settle to a steady-state situation. Although it is clear from the calculations that the hysteresis is not a purely kinetic phenomenon, the position of the transitions τ_B and τ_S does, however, depend on the length of the time interval T_c used in the ramping integration: in principle a very long time is needed so that, at every value of the parameter, the system is arbitrarily close to the steady state. In practice, however, the numerical method used in this simulation (Wolfram Research, Inc., 1993) does not allow an arbitrarily small stepsize, hence the integration time is limited to reasonable values. In the corresponding figures presented hereafter, transitions at higher pressures could not be calculated accurately because of excessively long scanning times. Due to this limitation, the figures representing the hysteresis transitions in the control parameter space actually reflect an artefact of the calculations. This artefact comes from the increasing time necessary to approach the steady state. This has, as a consequence, an artificial broadening of the hysteresis region. This effect is more pronounced at higher reactant pressures.

The steps involved in the calculations are shown in Figure 3, which shows the procedure used to generate Figures 4 to 6 as well as the transition points in Figures 7 to 9. Initial values of the system variables are coverages set to zero and partial pressures set to the corresponding inlet values.

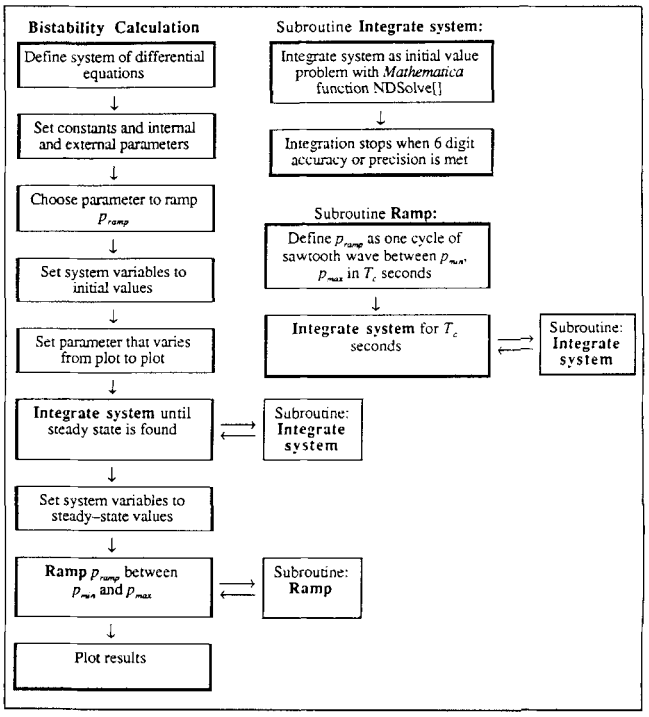

Figure 3. Steps taken for the calculations of Figures 4 to 6.

Results

There are potentially several kinetic models based on the mechanism (Figure 1), the difference coming from the values

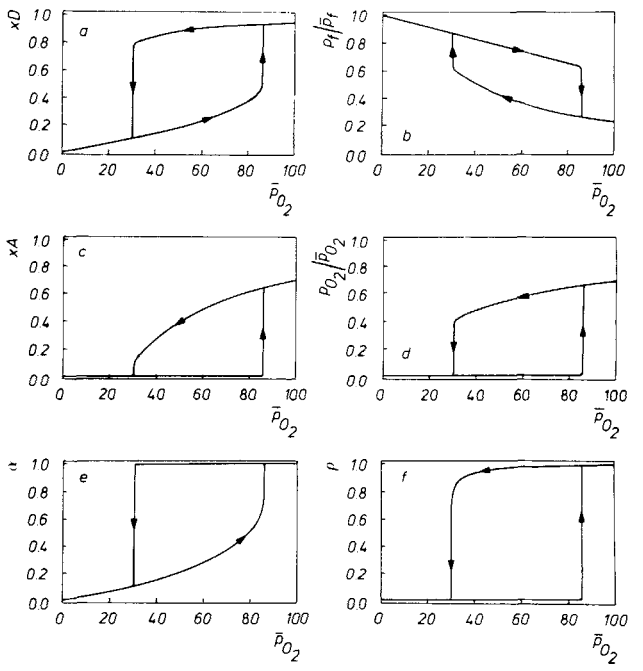

Figure 4. Typical results of a parameter ramping simulation: monostable and bistable regions.

Oxygen feed pressure was slowly varied between 0.01 and 100 torr in one complete ramping cycle taking 10^5 s. (a) through (e) show the behavior of the model variables, and (f) depicts the relative selectivity ρ of the reactor during the cycle. Except for (b), the hysteresis loops run counterclockwise. (For parameter values see Table 2.)

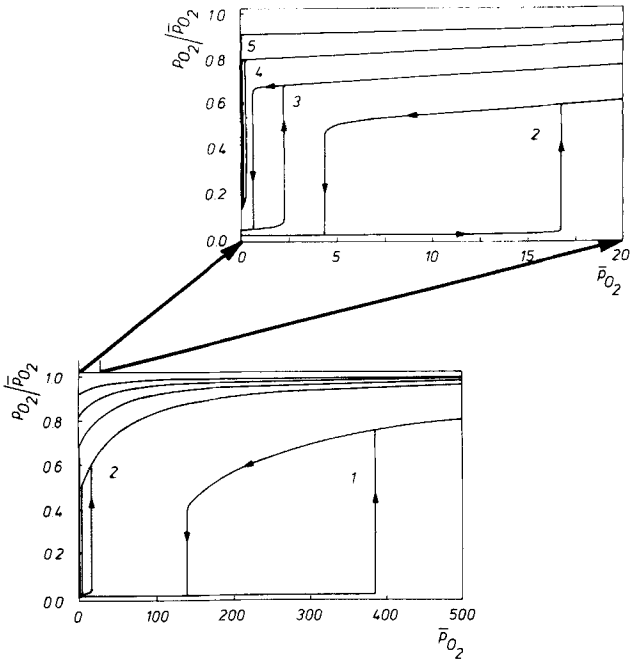

Figure 5. Simulations using oxygen feed pressure as the ramping parameter with several values of the reactant feed pressure.

The dependence of the hysteresis width and position on the reactant pressure is visible as a shift to lower oxygen pressures with a corresponding contraction of the bistability region. The hysteresis direction is counterclockwise in all cases. (For parameter values see Table 2.) For curves 1 to 5, hydrocarbon feed pressure $\bar{p}_f$ is, respectively, 2, 5, 10, 20, and 100.

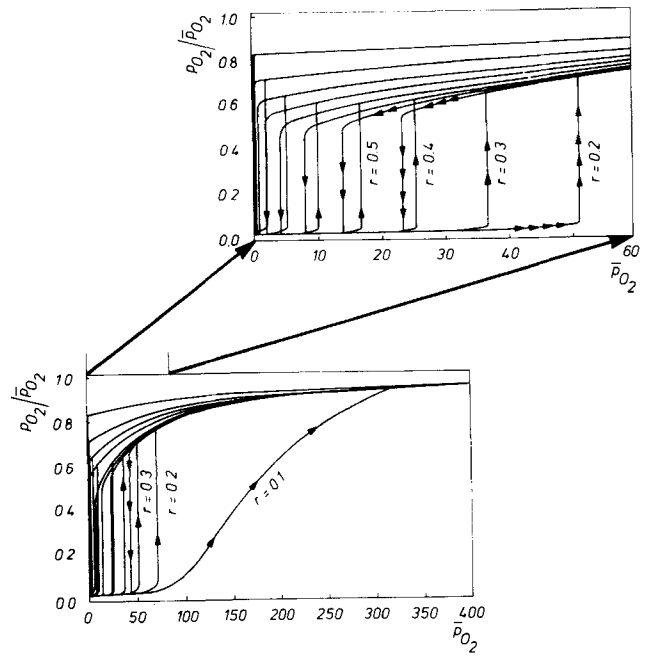

Figure 6. Simulations using oxygen feed pressure as the ramping parameter with several values of the catalyst composition r.

r = 0.1, 0.2, 0.3, 0.4, 0.5, 0.6, 0.7, 0.8, 0.9, 0.99. For parameter values see Table 2.

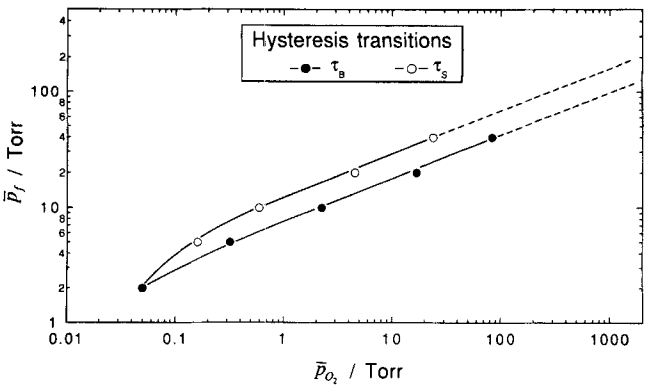

Figure 7. Bistability phenomena obtained by ramping the feed oxygen pressure at different feed reactant pressures.

Transitions at high oxygen pressures are indicated by dashed lines because calculations become increasingly inaccurate here. (For parameter values see Table 2.) r = 0.5.

assumed for reaction orders. For the model presented here, we selected the simplest hypothesis for the remote control loop (lower part of Figure 1). With respect to the catalytic loop, the nonselective reaction uses more oxygen (to form CO_2 and H_2O) than the selective reaction. This leads to the formation of nonselective sites for low $\bar{p}_{O_2}$.

The following model constitutes one of the simplest cases leading to bistability, namely that corresponding to the following values $m_1 = 1$, $m_2 = 1$, $m_3 = 2$, $m_4 = 1$. A model with $m_1 = 1$, $m_2 = 2$, $m_3 = 2$, $m_4 = 1$ also gave bistability regions.

The values of the parameters used for obtaining the results presented in the following figures are presented in Table 1. Model parameters used in the figures are presented in Table 2.

Figure 4 shows the variation of the main variables with change in oxygen pressure at the reactor inlet. Figures 4b and 4d give the ratios outlet/inlet for the hydrocarbon reactant and oxygen, respectively. Most striking is the change of selectivity (Figure 4f) with a wide region of inlet oxygen pressure where the reactor can be either very selective or nonselective. The corresponding variations of spillover oxy-

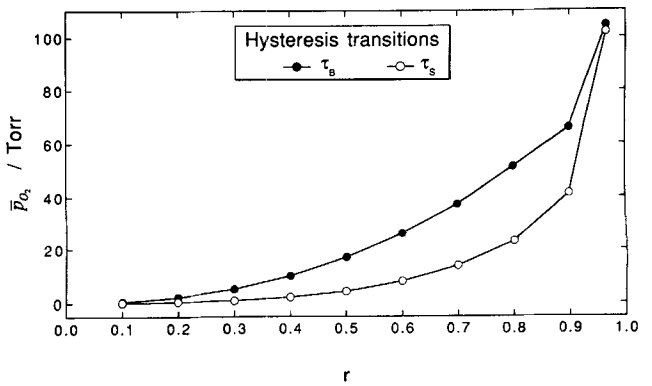

Figure 8. Transition points τ_B (point at which nonselective state becomes unstable) and τ_s (point at which selective state becomes unstable) for different compositions of the catalyst (r) as a function of inlet oxygen pressure $\bar{p}_{O_2}$.

For parameter values see Table 2.

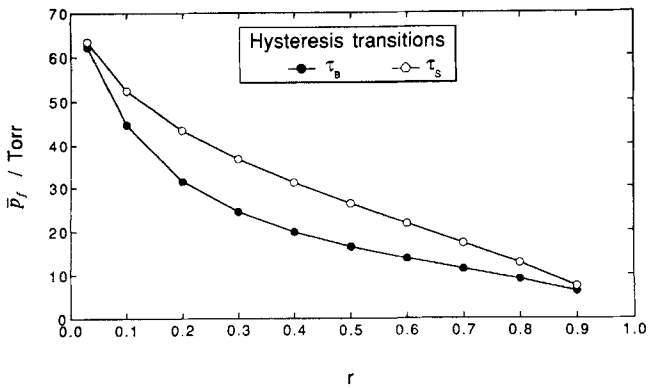

Figure 9. Transition points τ_B (point at which nonselective state becomes unstable) and τ_S (point at which selective state becomes unstable) for different compositions of the catalyst (r) as a function of inlet hydrocarbon reactant pressure $\bar{p}_f$.

For parameter values see Table 2.

gen coverage on donor and acceptor are given in Figures 4a and 4c, respectively. The shape of Figure 4e (fraction α of potential sites in the selective state) is not identical to that of Figure 4f (selectivity) because the catalytic activity is equal to the number of active sites multiplied by the rate constant (assumed to be different for the S and B reactions), and the orders with respect to oxygen are different. The more abrupt rise of selectivity, compared to α, is mainly due to the order of the selective reaction with respect to oxygen ($m_2 = 2$).

An overall view of the variations in the shape of the hysteresis loops are given in Figures 5 and 6; the variable parameter is hydrocarbon reactant inlet pressure $\bar{p}_f$ and catalyst composition r, respectively.

Figure 7 gives the inlet values ($\bar{p}_f$,$\bar{p}_{O_2}$) for which transitions between the two bistable states are observed, for $r = 0.5$. The transition points forming the boundaries of the bistable region show a dependence on the oxygen pressure similar to that obtained in a mathematical model for CO oxidation assuming a Langmuir-Hinshelwood mechanism. The variation of these transition values as a function of r and $\bar{p}_{O_2}$, and r and $\bar{p}_f$, are given in Figures 8 and 9, respectively. Bistabilities can occur in a wide range of catalyst composition r.

Figure 10 suggests the way the hysteresis width Δ, defined as the reactant or oxygen pressure difference between transition points, changes when various kinetic parameters change.

Table 1. Values of Model Parameters and Constants Used in the Calculations

External Reactor Parameters			Numerical Constants	
Symbol	Value	Units		
F	10	L/s	m_1	1
$\bar{p}_f$	(varies)	torr	m_2	1
$\bar{p}_{O_2}$	(varies)	torr	m_3	2
V	1	L	m_4	1
			N_B	6
			N_S	1

Internal Reactor Parameters			Rate Constants		
Symbol	Value	Units	Symbol	Value	Units
a	1	$1/cm^2$	k_a	9,420	g/s
Q	1	—	k_a^-	0.07	g/torr·s
r	(varies)	—	k_d	3.162	g/torr·cm^2·s
σ_A	1	cm^2/g	k_d^-	0.032	g/cm^2·s
σ_D	1	cm^2/g	k_B	1	[g/torr$^{m_3+m_4}$·s]
			k_S	1	[g/torr$^{m_1+m_2}$·s]
			k_t	5	g^2/cm^4·s

Table 2. Model Parameters Used in the Figures

Fig.	Oxygen Inlet $\bar{p}_{O_2}$	Reactant Inlet $\bar{p}_f$	Catalyst Composition r
3	Ramped	40 torr	0.5
4	Ramped	2, 5, 10, 14, 20, 40 torr	0.5
5	Ramped	20 torr	0.1, 0.2, ..., 0.9, 0.965
6	Ramped	2, 5, 10, 14, 20, 40 torr	0.5
7	Ramped	20 torr	0.1, 0.2, ..., 0.9, 0.965
8	10 torr	Ramped	0.03, 0.1, 0.2, ..., 0.9
9	Ramped	40 torr	0.5

Discussion

The comprehensive model presented here shows that reac-

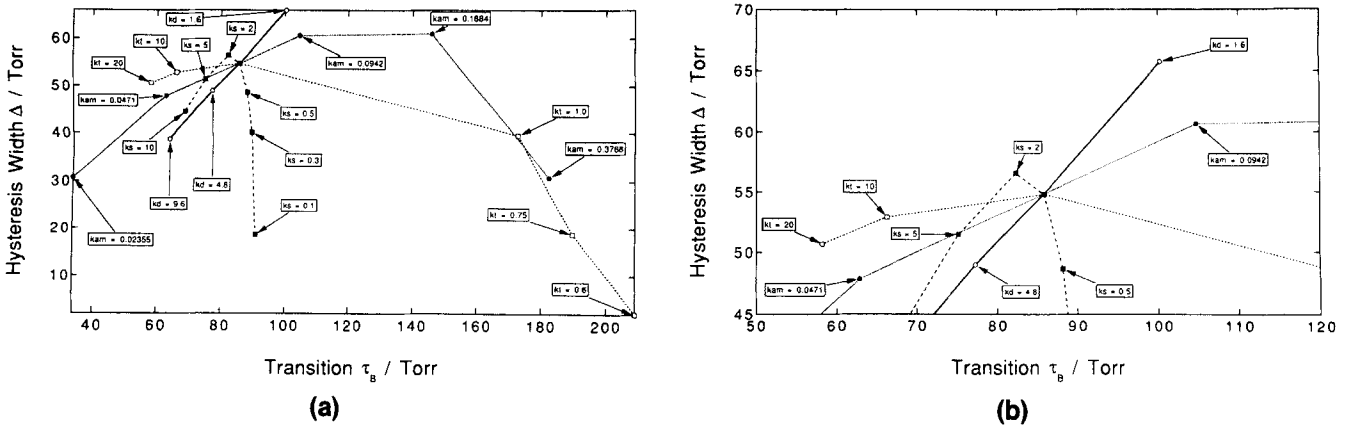

Figure 10. Changes of bistability phenomena found by varying important rate constants.

(a) and (b) correspond to different scales. Variations are started from the values summarized in Table 2. Note the sensitive dependence of the width of the bistable region on the rate constant k_S, which controls the selective reaction rate.

tions corresponding to a remote control mechanism can exhibit bistabilities. This confirms the earlier prediction of Delmon and Matralis (1991). It should be underlined that such a phenomenon is found in a model for *isothermal* conditions. The conclusion is that bistabilities in catalytic oxidation can occur without exhibiting any different thermal regimes, contrary to what has been generally accepted until now. As, in practice, catalytic oxidations are never perfectly isothermal, the question is left open whether a cooperation between both causes of bistability, namely nonisothermicity and remote control, could have significant consequences.

This article outlines the case where such isothermal bistabilities could occur. The question arises of the real catalytic reactions that could be candidates for the occurrence of such bistabilities. Contrary to hydrodesulfurization and hydrotreating on sulfide catalysts, no attempt has been made yet to determine the exact kinetics of remote-controlled oxidation reactions. The reaction order with respect to oxygen is not precisely known, as the overall apparent order determined until now includes the remote control effect (thus leading to noninteger apparent order). It is therefore difficult to predict the specific selective oxidation reaction where such bistabilities could occur. The low overall value of the oxygen order in remote-controlled allylic oxidation (Weng and Delmon, 1992) makes them unlikely candidates. The selective oxidation of butane to maleic anhydride consumes three oxygen molecules per butane molecule and seems very sensitive to oxygen pressure. It therefore seems to be a more reasonable candidate. As indicated in the introduction, it is precisely in this reaction that spectacular catastrophic losses of selectivity have been observed both in the laboratory and in industry.

Another question is whether a special kinetic behavior due to the bistability phenomena described here could be observed in other situations. It is known in the field of heterogeneous catalysis kinetics that phenomena, in particular material balance, must be considered at all scales (reactor, pellet, pore, nanometer surface area). In a sense, the continuously stirred tank flow reactor constitutes a basic model for reactor kinetics at the scale of a pore or of a nanometer scale surface area. One can thus reason that phenomena at large scales (reactions in pellets, in reactors) can be considered as the addition of numerous elementary "continuously stirred tank flow reactors" (cell models). If so, remote control could give rise to local instabilities, and even, possibly, to a chaotic behavior of different parts, due to inhomogeneity in catalyst composition, or to fluctuations in composition of the fluid phase, which produce stability transitions at different times.

In exploring variants of the model, we come to the conclusion that, in principle, the remote control could bring about sustained oscillations. However, the reaction orders and the values of the elementary rate constants that should be assumed for obtaining such an effect seem unrealistic, and the experimental field in which they should occur is extremely narrow. At the present stage of our work, it thus seems rather unlikely that oscillations could occur in reactions corresponding to models similar to the present one. This conclusion is valid for a perfectly homogeneous distribution of reactants and catalyst components, but may not be true if composition gradients are present or occur.

Acknowledgments

This work was made possible thanks to a Research Award (Forschungspreis) of the Alexander von Humbolt Foundation to one of the authors (B.D.). It is also part of a cooperative project in the frame of the European Community Programme: Human Capital and Mobility.

Notation

A = unoccupied site on acceptor catalyst
F = gas flow rate through reactor, L/s
k_a = rate constant for activation of deactivated sites on the acceptor phase g/s
k_a^- = rate constant for deactivation of sites active for the selective reaction on the acceptor phase, g/torr·s
k_B = rate constant for nonselective reaction of reactant M with oxygen at unoccupied acceptor sites B, g/torr$^{m_3+m_4}$·s
k_d = rate constant for dissociative adsorbtion of oxygen onto the donor catalyst surface, g/torr·cm^2·s
k_d^- = rate constant for recombination of adsorbed oxygen and desorption to the gas phase, g/cm^2·s
k_S = rate constant for selective reaction of reactant M with oxygen at unoccupied acceptor sites S, g/torr$^{m_1+m_2}$·s
k_t = rate constant for transfer of surface mobile oxygen between donor and acceptor catalyst, g^2/cm^4·s
OA = spillover oxygen on acceptor surface
R_a = activation rate, L/s
R_a^- = deactivation rate, L/s
R_B = nonselective reaction rate, torr/s
R_d = dissociation rate of molecular oxygen to surface mobile oxygen, L/s
R_d^- = recombination rate of adsorbed oxygen to molecular oxygen, L/s
R_S = selective reaction rate, torr/s
R_t = transfer rate of surface mobile oxygen betweeen donor and acceptor catalyst, L/s
V = volume of reactor, L
ρ = relative selectivity of the reactor $= R_S/(R_S + R_B)$

Literature Cited

Delmon, B., Process for Fabrication of Benzaldehyde from Toluene, Fr 1,568,763 (Apr. 21 1969); U.S. 3579,589 (May 18, 1971).

Delmon, B., and H. Matralis, "The Remote Control Mechanism. General Phenomena, Possible Consequences Concerning Unsteady State Processes," *Unsteady State Processes in Catalysis*, Yu. S. Matros, ed., USP, Utrecht, The Netherlands, p. 25 (1991).

Delmon, B., "The Control of Selectivity and Stability of Catalysts by Spillover Processes," in *New Aspects of Spillover in Catalysis*, T. Inui, K. Fujimoto, T. Uchijima, and M. Masai, eds., Elsevier, Amsterdam, p. 1 (1993).

Melo Faus, F., B. Zhou, H. Matralis, and B. Delmon, "Catalytic Cooperation between MoO_3 and Sb_2O_4 in N-Ethyl-Formamide Dehydration: III. Comparison of a Mathematical Model Based on the Remote Control Mechanism with Experimental Results," *J. Catal.*, **132**, 200 (1991).

Weng, L.-T., and B. Delmon, "Phase Cooperation and Remote Control Effects in Selective Oxidation Catalysts," *Appl. Catal.*, **81**, 141 (1992).

Wolfram Research Inc., *Mathematica*, Version 2.1, Wolfram Research Inc., Stanford, CA (1993).

Zhou, B., E. Sham, T. Machej, P. Bertrand, P. Ruiz, and B. Delmon, "Catalytic Cooperation between MoO_3 and Sb_2O_4 in N-Ethyl-Formamide Dehydration: I. Preparation, Characterization and Catalytic Results," *J. Catal.*, **132**, 157 (1991a).

Zhou, B., T. Machej, P. Ruiz, and B. Delmon, "Catalytic Cooperation between MoO_3 and Sb_2O_4 in N-Ethyl-Formamide Dehydration: II. Nature of Active Sites and Role of Spill-over Oxygen," *J. Catal.*, **132**, 183 (1991b).

Manuscript received Apr. 4, 1994, and revision received Sept. 15, 1994.